Current Biology

Volume 25
Number 4

February 16, 2015

www.cell.com

An Eye with 12 Retinas

Please cite this article in press as: Baldwin Fergus et al., A Unique Apposition Compound Eye in the Mesopelagic Hyperiid Amphipod *Paraphronima gracilis*, Current Biology (2015), http://dx.doi.org/10.1016/j.cub.2014.12.010

Current Biology *25*, 1–6, February 16, 2015 ©2015 Elsevier Ltd All rights reserved http://dx.doi.org/10.1016/j.cub.2014.12.010

Report

A Unique Apposition Compound Eye in the Mesopelagic Hyperiid Amphipod *Paraphronima gracilis*

Jamie L. Baldwin Fergus,[1,*] Sönke Johnsen,[2] and Karen J. Osborn[1]

[1]Department of Invertebrate Zoology, National Museum of Natural History, Smithsonian Institution, Washington, DC 20013, USA

[2]Department of Biology, Duke University, Durham, NC 27708, USA

Summary

The mesopelagic habitat is a vast space that lacks physical landmarks and is structured by depth, light penetration, and horizontal currents. Solar illumination is visible in the upper 1,000 m of the ocean, becoming dimmer and spectrally filtered with depth—generating a nearly monochromatic blue light field [1]. The struggle to perceive dim downwelling light and bioluminescent sources and the need to remain unseen generate contrasting selective pressures on the eyes of mesopelagic inhabitants [2]. Hyperiid amphipods are cosmopolitan members of the mesopelagic fauna with at least ten different eye configurations across the family—ranging from absent eyes in deep-living species to four enlarged eyes in mesopelagic individuals [3–7]. The hyperiid amphipod *Paraphronima gracilis* has a pair of bi-lobed apposition compound eyes, each with a large upward-looking portion and a small lateral-looking portion. The most unusual feature of the *P. gracilis* eye is that its upward-looking portion is resolved into a discontinuous retina with 12 distinct groups, each serving one transverse row of continuously spaced facets. On the basis of eye morphology, we estimated spatial acuity (2.5° ± 0.11°, SEM; n = 25) and optical sensitivity (30 ± 3.4 $\mu m^2 \cdot sr$, SEM; n = 25). Microspectrophotometry showed that spectral sensitivity of the eye peaked at 516 nm (±3.9 nm, SEM; n = 6), significantly offset from the peak of downwelling irradiance in the mesopelagic realm (480 nm). Modeling of spatial summation within the linear retinal groups showed that it boosts sensitivity with less cost to spatial acuity than more typical configurations.

Results and Discussion

The mesopelagic habitat exerts pressure on inhabitants to see, without being seen; often, these animals attempt to hide in plain sight while relying on vision for food capture, mate location, or predator avoidance. In these, efforts are made to maximize vision in dim light without having overly conspicuous eyes. In *Paraphronima*, long, transparent light guides carry light from the tightly packed crystalline cones to small, discontinuous retinas. This type of eye design has not been described previously, and its function is unknown. Here, we discuss the spectral sensitivity, eye morphology, spatial acuity, and light sensitivity of the eye of *Paraphronima gracilis* in addition to the potential advantages of a discontinuous retina.

*Correspondence: jamiebfergus@gmail.com

Eye Morphology

P. gracilis has a pair of bi-lobed apposition compound eyes consisting of a large upward-facing portion and smaller lateral-facing portion. The ommatidia of the upward-facing portion are arranged continuously in transverse rows across the eye and end in 12 discontinuous retinas (Figures 1 and 2). In the upward-facing portion of the dorsal eyes, a single ommatidium consisted of one crystalline cone connected to one fused rhabdom by a long light guide. Similar "fiber-optic"-type light guides are noted in the Phronimidae [8, 9]. The upward-facing portion of an eye was divided into 12 groups of ommatidia that formed rows perpendicular to the anterior-posterior axis of the animal (Figures 1 and 2). In each of the ten medial groups, nine ommatidia form a single row of ommatidia across the eye. The anterior-most and posterior-most groups had a higher density of ommatidia relative to medial retina groups. The anterior-most group had on average 22 ommatidia (±2, SEM; n = 11) arranged in approximately three rows. The posterior-most group had on average 21 ommatidia (±1, SEM; n = 11) also arranged in approximately three rows across the eye. The sensory portion of each ommatidium, the retinula, consisted of five retinular cells, and the inner, light-sensitive rhabdomeres of these five retinula cells form one fused rhabdom. Retinula arrangement appears constant across amphipods and fine details have been clearly resolved by electron microscopy in other hyperiid species [5, 8, 10].

Ommatidia in the lateral-facing portion of the eye were structurally similar to, but smaller than, the upward-facing ommatidia, bearing a single crystalline cone connected to the rhabdom by a light guide (Figures 1 and S1 and Table S1). There were, on average, 25 laterally directed ommatidia per eye (±1, SEM; n = 20). There was one large group of approximately 14 lateral and downward-looking ommatidia. Anterior to this large group, there were four groups of three lateral-looking ommatidia (Figures 1C and 1D).

Spectral Sensitivity

Microspectrophotometry data indicated a λ_{max} (wavelength of maximum absorbance) at 516 nm (±1.6 nm, SEM; n = 6 difference scans from four individuals). Mesopelagic animals searching visually for hosts, prey, or mates in the horizontal and downward planes will often have optimal spectral sensitivities near 480 nm [11], matched to the most prevalent wavelengths in the dim, downwelling light and corresponding with maximal light levels. However, mesopelagic animals may have an easier time distinguishing overhead objects if the peak spectral sensitivity of their photoreceptors is slightly offset from the dominant wavelengths of the downwelling light [12]. The difference is due to the wavelength dependence of the attenuation of contrast on viewing angle. For pelagic animals looking upward, contrast attenuates most slowly with distance at approximately 515 nm [12]. Thus, our microspectrophotometry (MSP) suggests that *P. gracilis* may be most adept at searching overhead for hosts, prey, or mates silhouetted against downwelling light. This benefit of increased sighting distance comes at the cost of being 15%–25% less sensitive to the shorter wavelengths of light most prevalent in the mesopelagic habitat.

Please cite this article in press as: Baldwin Fergus et al., A Unique Apposition Compound Eye in the Mesopelagic Hyperiid Amphipod *Paraphronima gracilis*, Current Biology (2015), http://dx.doi.org/10.1016/j.cub.2014.12.010

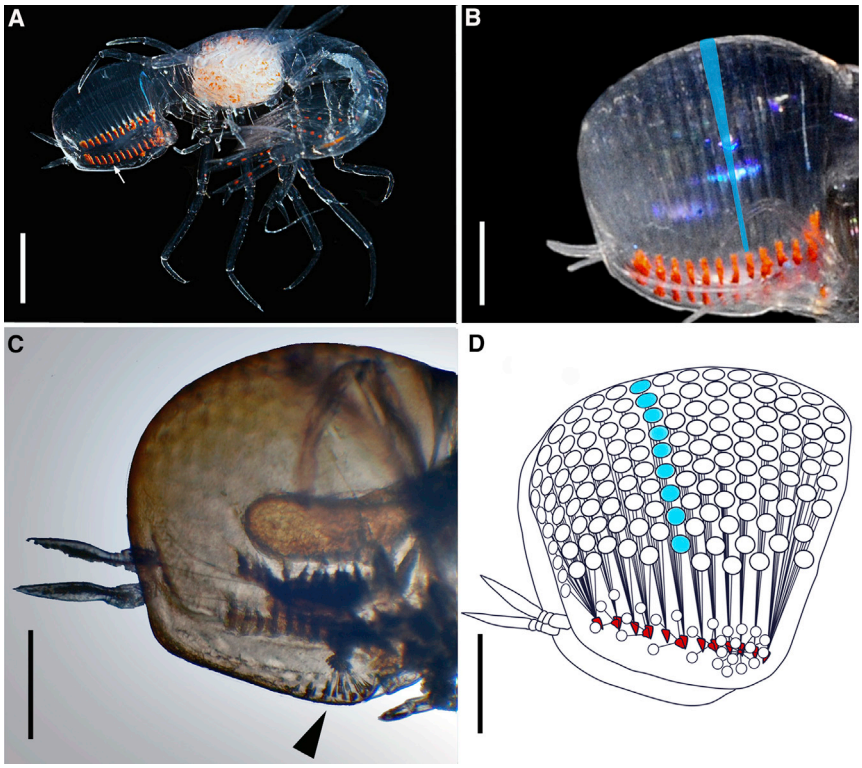

Figure 1. Photographs and Schematic Diagrams of the eyes of *P. gracilis*

(A) Ventral-lateral view of a gravid female *P. gracilis*. Eggs are visible as a white mass in the brood pouch. The white arrow indicates the photosensory portion of an ommatidial group. The red/orange coloration is from screening pigments located within and around the retinula cells contributing to the fused rhabdom of each ommatidia. The scale bar represents 2 mm.

(B) Lateral view of *P. gracilis*. Facets and light guides are nearly transparent in live specimens; here, the path of an ommatidium is highlighted in blue. The scale bar represents 1 mm.

(C) Photograph of the ventrolateral view of a fixed *P. gracilis* head. The arrow indicates the lateral eye. The scale bar represents 1 mm.

(D) Illustration of one bi-lobed eye showing the facets (open circles) connected to groups of rhabdoms (red/orange) by long light guides (black lines). Lateral-facing ommatidia (smaller circles) are also illustrated. The rhabdoms of the five groups of lateral-facing ommatidia are positioned near the dorsal group, but are physically separate. The scale bar represents 1 mm.

See also Figure S1.

Spatial Acuity

Calculations of spatial acuity and light sensitivity were based on morphological measurements (Tables 1 and S1). Facet diameter and eye curvature may vary over the surface of a compound eye, contributing to areas of higher or lower spatial acuity. In *P. gracilis*, facet diameter was relatively constant, although the curvature of the eye varied slightly along the upward-facing surface. In the upward-facing eye, the estimate of interommatidial angle was approximately 1.2°. Acceptance angle was not significantly affected by diffraction, due to the relatively wide aperture of the crystalline cone, and was estimated at 2.5° (±0.11°, SEM; n = 25) assuming that focal length was equivalent to the average length of the crystalline cone (280 ± 11 μm, SEM; n = 25). In the lateral-facing portion of the eye, the acceptance angles were 5.5° (±0.3°, SEM; n = 25). In previous studies, pseudopupil measurements have been used to accurately measure interommatidial angle and would be beneficial here in confirming our morphological approximations of spatial acuity [9, 13].

The estimates of acceptance angle and interommatidial angle for *P. gracilis* were similar to other values found for other hyperiid amphipods [9, 13]. The $\Delta\rho$:$\Delta\phi$ ratio, describing the amount of overlap of the receptive fields of adjacent photoreceptors [14–16], was as great as 2.3 in *P. gracilis*. In diurnal animals, the ratio is often close to 1, but for crepuscular, nocturnal, or mesopelagic animals, $\Delta\rho$ may be much greater than $\Delta\phi$, indicating an overlap of visual fields [14–16]. This type of overlap increases light capture and thus increases the reliability of the signal by raising the signal to noise ratio—at the cost of spatial resolution [14–17]. In hyperiids with known $\Delta\rho$:$\Delta\phi$, including *Paraphronima*, the upward-looking eyes tend to have higher ratios, which have been attributed to the need for detecting low-contrast objects against unstructured backgrounds [9–13].

Light Sensitivity

The optical sensitivity of the upward-facing portion of the eye was 32 $\mu m^2 \cdot$ sr (±3.4, SEM; n = 25). In the lateral eye, sensitivity was 74 $\mu m^2 \cdot$ sr (±6.7, SEM; n = 25). *Paraphronima*'s visual sensitivity values are comparable to nocturnal or crepuscular animals such as moths or dung-beetles [18], as well as other mesopelagic hyperiids [13]. In all eyes, there is a tradeoff between light sensitivity and resolution. Eyes that are much more sensitive than *P. gracilis*'s are found in benthic and bathypelagic crustaceans such as the isopod *Cirolana* and the shrimp *Oplophorus* (3,300 and 4,200 $\mu m^2 \cdot$ sr, respectively); however, these animals have extremely poor spatial acuity as a result of their need to gather light in the exceptionally low-light environment of the deep ocean [18]. Sensitivity in diurnal animals functioning under high light levels tends to be much lower, usually below 0.5 $\mu m^2 \cdot$ sr [18]; here, the amount of light is not limited, and animals need not sacrifice acuity for sensitivity. The sensitivity values found in *P. gracilis* indicate that vision in this species is suited for dim light in the mesopelagic habitat and for detecting targets against a non-structured background.

The smaller lateral portion of the *P. gracilis* eye has lower spatial resolution (5.7°) and higher light sensitivity (74 $\mu m^2 \cdot$ sr) and most likely functions as a bioluminescence detector. The facets are aimed both horizontally and downward and may have a much larger field of view than the dorsal eyes. The specific conditions under which *Paraphronima* can detect bioluminescence will depend on several factors, including the spectral peak and number of photons produced by the bioluminescence emission, the amount of background light, and the distance over which the signal is traveling to the viewer [19]. Generally, if the lateral eyes are following the predictions given by Land [20], those of *P. gracilis* are likely to be better suited for detecting bioluminescent sources compared to the upward-facing eye.

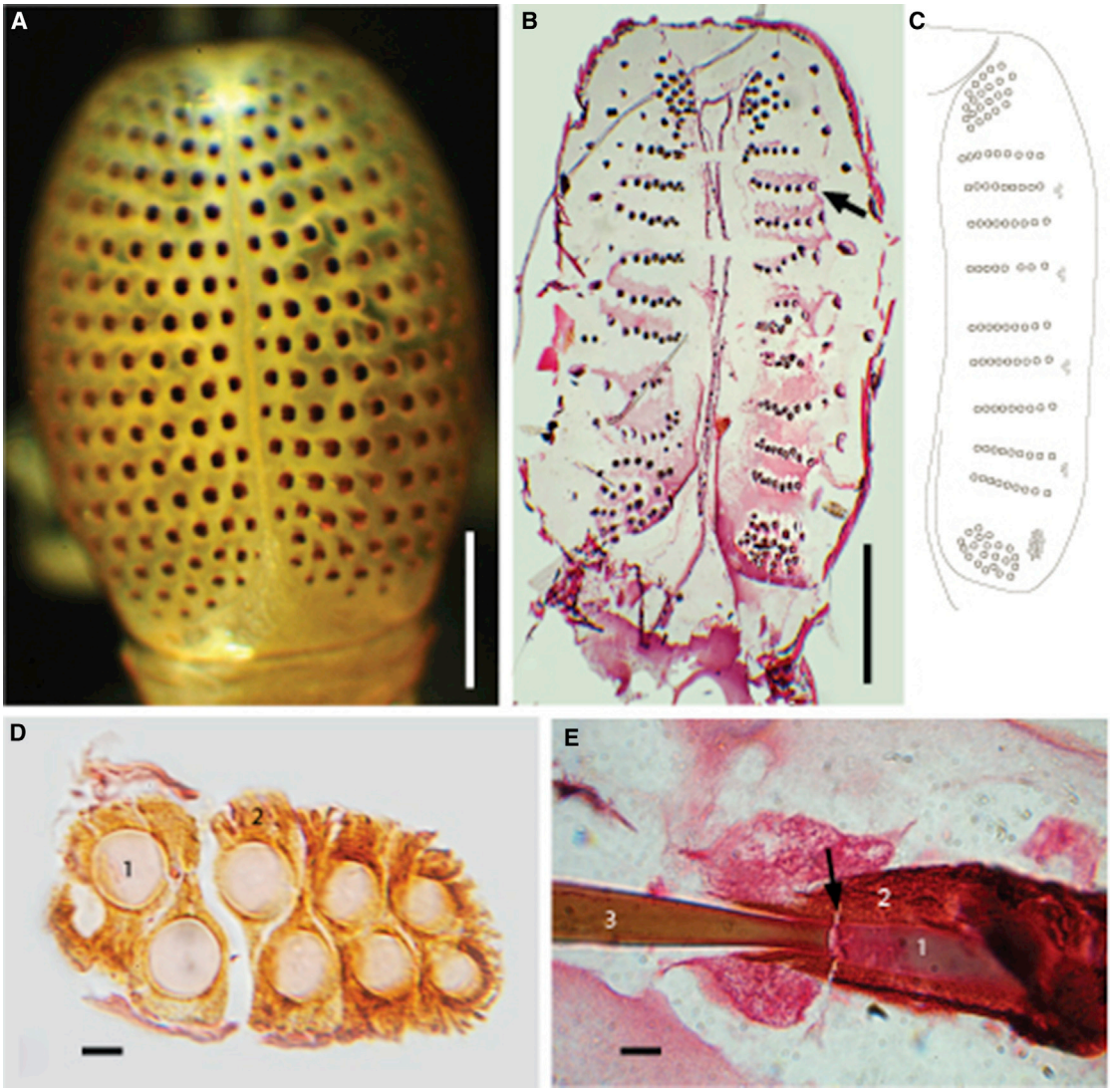

Figure 2. The Eyes of *P. gracilis*

(A) Dorsal view showing the facets of the eyes in an older, fixed sample. The scale bar represents 1 mm.

(B) Transverse section from approximately midway through the eye showing the organization of the light guides, which are the small, dark-colored circles in distinct groups that fan across the eye. The arrow indicates one row of light guides. The scale bar represents 1 mm.

(C) Schematic diagram illustrating the organization of ommatidia in the transverse plane midway through the eye.

(D) Transverse section of one dorsally directed retina group. Rhabdoms (1) are surrounded by retinula cells (2). The scale bar represents 10 μm.

(E) Sagittal section showing the connection of the light guide (3) to the fused rhabdom (1) surrounded by retinula cells (2). The intersection of light guide and rhabdom is marked with an arrow. The scale bar represents 10 μm. For excellent drawings of similar structures in *Phronima*, see [8].

See also Figure S2.

Function of the Discontinuous Retina

We have considered several possible advantages of a discontinuous retina over a single, continuous retinal sheet found in typical apposition compound eyes. Initially, we considered that a discontinuous retina was a method of camouflage or reducing the visibility of the retina. However, the discontinuous retina could be viewed by animals with high spatial acuity as two dark, dashed lines among a relatively clear body. To animals with lower spatial acuity, the discontinuous retinas would most likely be seen as one blurry mass. In either scenario, the pigments of the retina may be no more or less visible than a single retinal sheet.

Another possibility is that *Paraphronima* may be using their unique retinal configuration, paired with neural adaptations, to use spatial summation to operate under changing light conditions. *Paraphronima* may boost sensitivity by summing within a retinal group. Under this scenario, each retinal group would act as a single, crude pixel. Light sensitivity in the medial twn retinal groups would increase 9-fold with signal summation (234 $\mu m^2 \cdot sr$). Under this scenario, acuity would be reduced to about 12.1°, but only in the lateral axis. Spatial acuity would remain 2.5° in the anterior-posterior axis, as the rows of ommatidia are arranged in a 1 × 9 formation. Frequently, animals that use spatial summation sum a light signal over a circlular or square cluster of ommatidia [21]. The typical summing of nine ommatidia would result in 3 × 3 pattern. Both arrangements would boost the light signal, but they result in a different image. Figure 3 illustrates how *Paraphronima* may view a prey

Please cite this article in press as: Baldwin Fergus et al., A Unique Apposition Compound Eye in the Mesopelagic Hyperiid Amphipod *Paraphronima gracilis*, Current Biology (2015), http://dx.doi.org/10.1016/j.cub.2014.12.010

Table 1. Calculations of Spatial Acuity and Light Sensitivity in the Bi-lobed Eyes of *P. gracilis*, Including SEM

Eye	*D* (μm)	Δρ (°)	Δø (°)	Δρ: Δø	λ_{max} (nm)	*S* (μm² · sr)
Dorsal	92 ± 2	2.5 ± 0.1	1.2 ± 0.1	2.1	516 ± 1.6	26 ± 3.4
Lateral	67 ± 2	5.7 ± 0.3	6.7 ± 0.5	0.85	516 ± 1.6	74 ± 6.7

D, facet diameter; Δρ, acceptance angle; Δø, interommatidial angle; λ_{max}, wavelength of maximum spectral sensitivity; *S*, optical sensitivity. See also Figure S3 and Table S1.

item (e.g., a calycophoran siphonophore) with and without spatial summation. Both summed images would be nine times brighter with spatial summation; however, the linear summation retains more detail in certain planes. Additionally, by summing along a single axis, *Paraphronima* could, in theory, line up the long axis of the target with the summed visual axis and in this way allow for a sharper image than those formed in two axes using a circular summation pattern [23]. A similar type of summation is seen in nocturnal bees living in a rainforest dominated by vertical tree trunks [23]. The 9-fold increase in light capture via spatial summation gives *Paraphronima* a 3-fold greater contrast sensitivity, thereby increasing the distance at which it can detect objects. It is possible that the summation is dynamic, changing in response to changing light levels associated with diel vertical migration, changes in water productivity, or changes in solar illumination [21]. Observations of live *Paraphronima* indicate that they are active at depths between roughly 150 and 500 m. Light levels change several orders of magnitude over this depth range and vision may thus benefit from spatial summation. A basis for spatial summation is also suggested in the hyperiid *Phronima* [9].

Conclusions

In hyperiids, sensory evolution is thought to be influenced by the need to detect hosts [24, 25], although in *Paraphronima* the pressure to locate both prey and mates may be equally influential. The spectral sensitivity of *Paraphronima* (λ_{max} = 516 ± 1.6 nm, SEM) is significantly offset from the predominant wavelength of downwelling light (480 nm), indicating an advantage for detecting overhead animals against dim downwelling light. The discontinuous retinas and transverse arrangement of the ommatidia suggest that spatial summation in a single axis allows *Paraphronima* to boost the light signal while minimizing loss in resolution in relevant planes. Further experiments designed to assess the visual physiology and ecology of these unique animals will assist in interpreting the adaptive function of the suite of remarkable structural peculiarities underlying an eye design that exists nowhere else in nature.

Experimental Procedures

Specimens of *P. gracilis* were collected by night trawls off the R/V *Western Flyer* operated by the Monterey Bay Aquarium Research Institute (MBARI) in the Monterey Submarine Canyon between a depth of 200 and 500 m (36° 32.0′ N, 122° 30.2′ W). Animals used for microspectrophotometry were transferred to individual light-tight containers filled with chilled seawater (6°C) and placed in a dark cold room (6°C) for 12 hr. Dark-adapted samples were stored at −80°C and were then transferred on dry ice to Duke University for analysis. Samples selected for morphological examination were fixed in 4% formaldehyde (diluted in seawater and buffered with borax) for a minimum of 48 hr.

Video observations recorded by the cameras of MBARI's remotely operated underwater vehicle (ROV) were reviewed after a search of the MBARI Video Annotation Reference System (VARS). Observations were reviewed for information regarding *Paraphronima*'s distribution and behavior.

Fifty specimens of *P. gracilis* from the Smithsonian Institution National Museum of Natural History collections were examined by light microscopy. Eleven freshly captured animals were embedded in paraffin, sectioned at 8 μm, processed, and stained with Picro-Ponceau [26]. Measurements including crystalline cone diameter (*D*) and length (*f*), light guide width and length, and rhabdom width (*d*) and length (*l*) were taken from the images using ImageJ (NIH).

Estimates of visual acuity were made using both interommatidial angle (Δø), the angle between adjacent ommatidial axes, and photoreceptor acceptance angle (Δρ), a combination of the rhabdom's angular capture cross-section and its modification by the diffraction of light. Estimates of interommatidial angle were made using the radius of curvature of the *P. gracilis* eye and the average diameter of the cones, taken as facet diameter because amphipods lack faceted lenses. Local curvature of the eye was estimated by fitting circles to images of eyes. Recognizing that apposition compound eyes are not perfectly spherical, with flattened areas tending to have higher resolution, we fit multiple circles to each image. The interommatidial angle (Δø) is the facet diameter (*D*) divided by the local radius of curvature of the eye (*R*):

$$\Delta\phi = \frac{D}{R}\ [15] \qquad \text{(Equation 1)}$$

This describes the separation between ommatidial axes, and this angle indicates how the overall image is sampled [18]. Snyder's model of spatial acuity [27] was used to estimate acceptance angle ($\Delta\rho$, the angle over which a rhabdom accepts light):

$$\Delta\rho = \sqrt{\left(\frac{d}{f}\right)^2 + \left(\frac{\lambda}{D}\right)^2}. \qquad \text{(Equation 2)}$$

Here, *d* is rhabdom diameter, *f* is focal length of the ommatidium, λ is wavelength of the incident light, and *D* is facet diameter. For λ, we used the dominant wavelength of light in the mesopelagic (480 nm) divided by the refractive index of the crystalline cone nearest the light guide (1.39) [9, 28]. The focal length was assumed to be the length of the crystalline cone, an assumption based on work in the hyperiid *Phronima sedentaria*, in whnich ray tracing determined focal length to be equivalent to the length of the crystalline cone [9].

The sensitivity, or light gathering ability *S* (μm² · sr), of an eye viewing monochromatic light is given by

$$S = \left(\frac{\pi}{4}\right)^2 D^2 \Delta\rho^2 \left(1 - e^{-kl}\right), \qquad \text{(Equation 3)}$$

where *k* is the coefficient of absorption of the rhabdom at the wavelength of the incident light, here taken as 0.0106 μm^{-1} on the basis of measurements from a deep-sea shrimp (*Sergestes*; [29]), and *l* is rhabdom length [14].

Spectral sensitivity was determined using MSP techniques similar to previously described methods [30, 31], using a custom-built, computer-controlled, single-beam, wavelength-scanning microspectrophotometer (see Figure S3).

Supplemental Information

Supplemental Information includes three figures and one table and can be found with this article online at http://dx.doi.org/10.1016/j.cub.2014.12.010.

Author Contributions

J.L.B.F. contributed histology, MSP experiments, MSP design and construction, analysis, modeling spatial acuity and sensitivity, and writing. S.J. contributed MSP design and construction, data analysis, modeling summation, and editing. K.J.O. contributed to field work, behavioral observations, depth distribution, illustrations, and editing.

Acknowledgments

We thank the crew of MBARI's R/V *Western Flyer* and Kyra Schlinning for assistance with video review and VARS searches. Drs. Barbara Carlsward and Paul Switzer provided laboratory and equipment space. Dr. Jon Norenburg provided histology training. Freya Goetz, Stephanie Bush, Kim Reisenbichler, Kris Walz, and Robert Sherlock provided assistance with specimen collection, and Drs. Bruce Robison and Steven Haddock provided

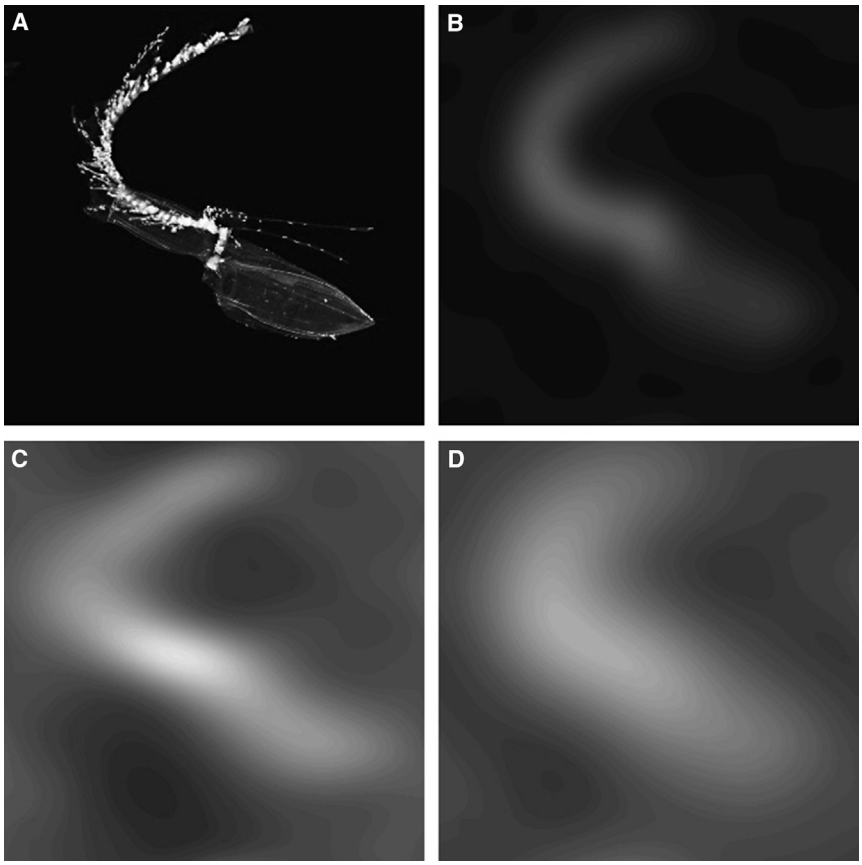

Figure 3. The Appearance of a Calychophoran Siphonophore, *Chuniphyes sp*., to the *P. gracilis* Eye with Natural Brightness and Spatial Summation

(A) Original image, assumed to be 5 cm in diameter and viewed from a distance of 14.4 cm, thus subtending an angle of 20°.

(B) The appearance of the siphonophore to the eye of *P. gracilis* without spatial summation (thus with an acceptance angle of 2.5°).

(C) The appearance of the siphonophore to the *P. gracilis* eye with summation in a single axis across nine ommatidia, giving an acceptance angle of 12.1° ($\Delta\rho$ / 2 + (9 − 1) · $\Delta\phi$ + $\Delta\rho$ / 2) in one axis and 2.5° in the perpendicular axis. Note that the image is nine times brighter than the image formed without spatial summation.

(D) The appearance of the siphonophore under the more typical type of spatial summation, where the signal is grouped within a circle or square of ommatidia. Here, nine ommatidia are summed in a square (3 × 3) pattern, giving an acceptance angle of 4.9° ($\Delta\rho$ / 2 + (3 − 1) · $\Delta\phi$ + $\Delta\rho$ / 2) in both axes. The image is again nine times brighter but is not as sharp as the image formed using linear summation.

The images in (B)–(D) were all created using Fourier methods. In brief, the Fourier transform of the image was multiplied by the modulation transfer function (MTF) of the eye, and then an inverse Fourier transform was performed to recover the image as it would appear to the eye. The MTF used, as a function of spatial frequency ν, was $MTF = e^{-3.56\nu^2(\Delta\rho)^2}$, where $\Delta\rho$ is the acceptance angle for the given summation condition [22]. In the linear summation case, $\Delta\rho$ varied between 12.1° and 2.5° in an elliptical manner.

invitations to participate in MBARI field expeditions. Thank you to Drs. William Browne and Daniel Speiser for commenting on early versions of the manuscript, as well as two anonymous reviewers. Rachel Goncalves drew the schematic of the MSP (Figure S3). J.B.F. was supported by a Peter Buck Postdoctoral Fellowship. S.J. was supported in part by a grant from the Office of Naval Research (N00014-09-1-1053).

Received: November 6, 2014
Revised: November 19, 2014
Accepted: December 2, 2014
Published: January 15, 2015

References

1. Jerlov, N.G. (1968). Optical Oceanography, *Volume 5* (Elsevier).
2. Warrant, E.J., and Locket, N.A. (2004). Vision in the deep sea. Biol. Rev. Camb. Philos. Soc. *79*, 671–712.
3. Vinogradov, M.E., Volkov, A.F., Semenova, T.N., and Siegel-Causey, D. (1996). Hyperiid Amphipods (Amphipoda, Hyperiidea) of the World Oceans (Smithsonian Institution Libraries).
4. Zeidler, W. (2009). A Review of the Hyperiidean Amphipod Superfamily Lanceoloidea Bowman & Gruner, 1973 (Crustacea: Amphipoda: Hyperiidea) (Magnolia Press).
5. Hallberg, E., Nilsson, H.L., and Elofsson, R. (1980). Classification of amphipod compound eyes–the fine structure of the ommatidial units (Crustaca, Amphipoda). Zoomorphologie *94*, 279–306.
6. Brusca, G.J. (1967). The ecology of pelagic Amphipoda, I. Species accounts, vertical zonation and migration of amphipods from the waters off southern California. Pac. Sci. *21*, 382–393.
7. Hurt, C., Haddock, S.H.D., and Browne, W.E. (2013). Molecular phylogenetic evidence for the reorganization of the Hyperiid amphipods, a diverse group of pelagic crustaceans. Mol. Phylogenet. Evol. *67*, 28–37.
8. Ball, E.E. (1977). Fine structure of the compound eyes of the midwater amphipod *Phronima* in relation to behavior and habitat. Tissue Cell *9*, 521–536.
9. Land, M.F. (1981). Optics of the eyes of *Phronima* and other deep sea amphipods. J. Comp. Physiol. *145*, 209–226.
10. Meyer-Rochow, V.B. (1978). The eyes of mesopelagic crustaceans. II. *Streetsia challengeri* (amphipoda). Cell Tissue Res. *186*, 337–349.
11. Douglas, R.H., Hunt, D.M., and Bowmaker, J.K. (2003). Spectral sensitivity tuning in the deep sea. In Sensory Processing in Aquatic Environments, S.P. Collins and N.J. Marshall, eds. (Springer), pp. 323–342.
12. Johnsen, S. (2014). Hide and seek in the open sea: pelagic camouflage and visual countermeasures. Annu. Rev. Mar. Sci. *6*, 369–392.
13. Land, M.F. (1989). The eyes of hyperiid amphipods: relations of optical structure to depth. J. Comp. Physiol. A *164*, 751–762.
14. Land, M.F. (1981). Optics and vision in invertebrates. In Handbook of Sensory Physiology, *Volume VII/6B*, Autrum, H., ed. (Springer), pp. 471–592.
15. Land, M.F. (1997). Visual acuity in insects. Annu. Rev. Entomol. *42*, 147–177.
16. Gonzalez-Bellido, P.T., Wardill, T.J., and Juusola, M. (2011). Compound eyes and retinal information processing in miniature dipteran species match their specific ecological demands. Proc. Natl. Acad. Sci. USA *108*, 4224–4229.
17. Warrant, E. (2004). Vision in the dimmest habitats on earth. J. Comp. Physiol. A Neuroethol. Sens. Neural Behav. Physiol. *190*, 765–789.
18. Land, M.F., and Nilsson, D.-E. (2012). Animal Eyes, Second Edition (Oxford University Press).
19. Nilsson, D.E., Warrant, E., and Johnsen, S. (2014). Computational visual ecology in the pelagic realm. Philos. Trans. R. Soc. Lond. B Biol. Sci. *369*, 20130038.
20. Land, M.F. (2000). On the functions of double eyes in midwater animals. Philos. Trans. R. Soc. Lond. B Biol. Sci. *355*, 1147–1150.

Please cite this article in press as: Baldwin Fergus et al., A Unique Apposition Compound Eye in the Mesopelagic Hyperiid Amphipod *Paraphronima gracilis*, Current Biology (2015), http://dx.doi.org/10.1016/j.cub.2014.12.010

21. Warrant, E.J. (1999). Seeing better at night: life style, eye design and the optimum strategy of spatial and temporal summation. Vision Res. *39*, 1611–1630.
22. Cronin, T.W., Johnsen, S., Marshall, N.J., and Warrant, E.J. (2014). Visual Ecology (Princeton University Press).
23. Klaus, A., and Warrant, E.J. (2009). Optimum spatiotemporal receptive fields for vision in dim light. J. Vis. *9*, 1–16.
24. Laval, P. (1980). Hyperiid ampipods as crustacean parasitoids associated with gelatinous zooplankton. Oceanogr. Mar. Biol. Annu. Rev. *18*, 11–56.
25. Harbison, G.R., Biggs, D.C., and Madin, L.P. (1977). The associations of Amphipoda Hyperiidea with gelatinous zooplankton—II. Associations with Cnidaria, Ctenophora and Radiolaria. Deep Sea Res. *24*, 465–488.
26. Kier, W. (1992). Hydrostatic skeletons and muscular hysdrostats. Biomechanics (Structures and Systems): A Practical Approach (TRL Press at Oxford University Press).
27. Snyder, A.W. (1979). Physics of vision in compound eyes. In Handbook of Sensory Physiology, *Volume VII/6A*, Autrum, H., ed. (Springer), pp. 225–313.
28. Li, L., Stramski, D., and Reynolds, R.A. (2014). Characterization of the solar light field within the ocean mesopelagic zone based on radiative transfer simulations. Deep Sea Res. Part I Oceanogr. Res. Pap. *87*, 53–69.
29. Hiller-Adams, P., Widder, E.A., and Case, J.F. (1988). The visual pigments of four deep-sea crustacean species. J. Comp. Physiol. A Neuroethol. Sens. Neural Behav. Physiol. *163*, 63–72.
30. Loew, E.R. (1994). A third, ultraviolet-sensitive, visual pigment in the Tokay gecko (*Gekko gekko*). Vision Res. *34*, 1427–1431.
31. Provencio, I., Loew, E.R., and Foster, R.G. (1992). Vitamin A_2-based visual pigments in fully terrestrial vertebrates. Vision Res. *32*, 2201–2208.

Current Biology

Supplemental Information

A Unique Apposition Compound Eye in the Mesopelagic Hyperiid Amphipod *Paraphronima gracilis*

Jamie L. Baldwin Fergus, Sönke Johnsen, and Karen J. Osborn

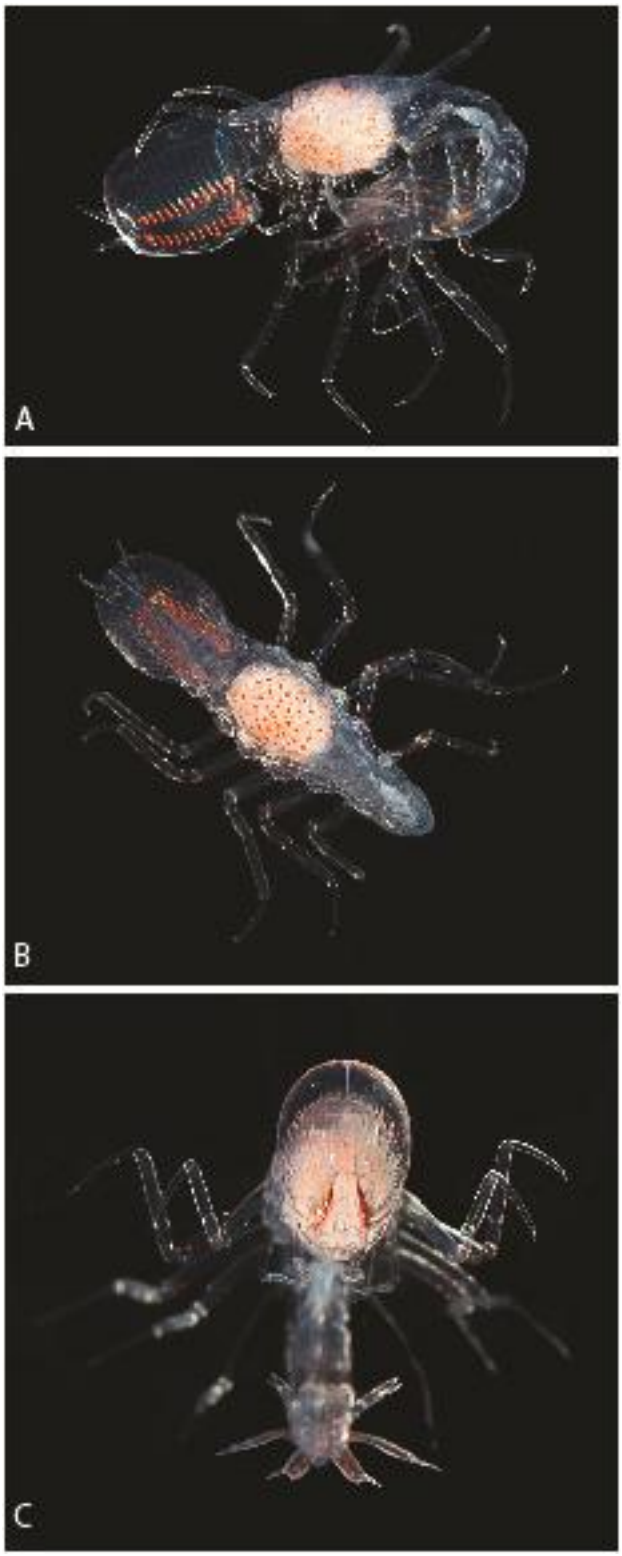

Figure S1, Related to Figure 1. Live *Paraphronima gracilis* photographed onboard the R/V *Western Flyer* with a Canon EOS 5D. A. Ventrolateral view, showing the large proportion of the body taken up by the eyes and the two rows of discontinuous retinas. B. Dorsal view, showing facets of the dorsally directed ommatidia. C. Anteroventral view, showing the transparent body and the fan of light guides radiating from each retina. Prominent opaque mass visible in all shots is a large egg mass.

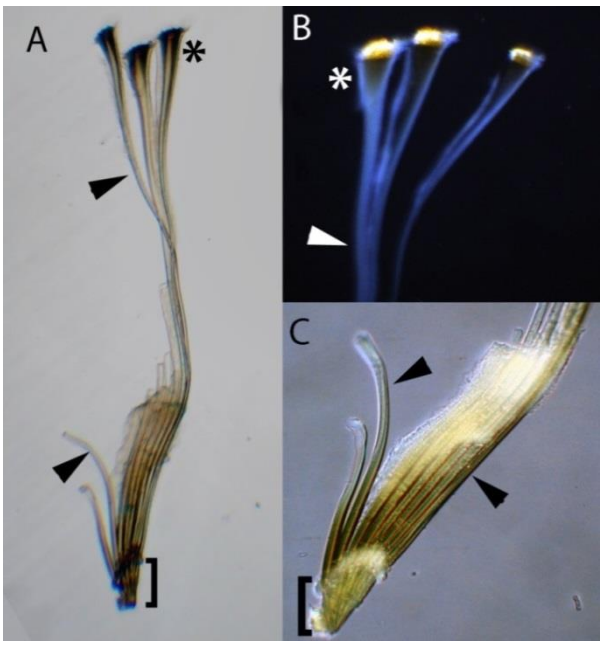

Figure S2, Related to Figure 2. Whole ommatidia dissected from the dorsal eye of *Paraphronima gracilis.* A. Group of ommatidia dissected from *P. gracilis*. Three of nine ommatidia remain intact. B. Crystalline cones of *P. gracilis* (dark field). C. The base of the ommatidia group where photoreceptors and light guides join in a fan shape. Asterisks indicate crystalline cones. Arrows indicate selected light guides. Brackets highlight a group of rhabdoms.

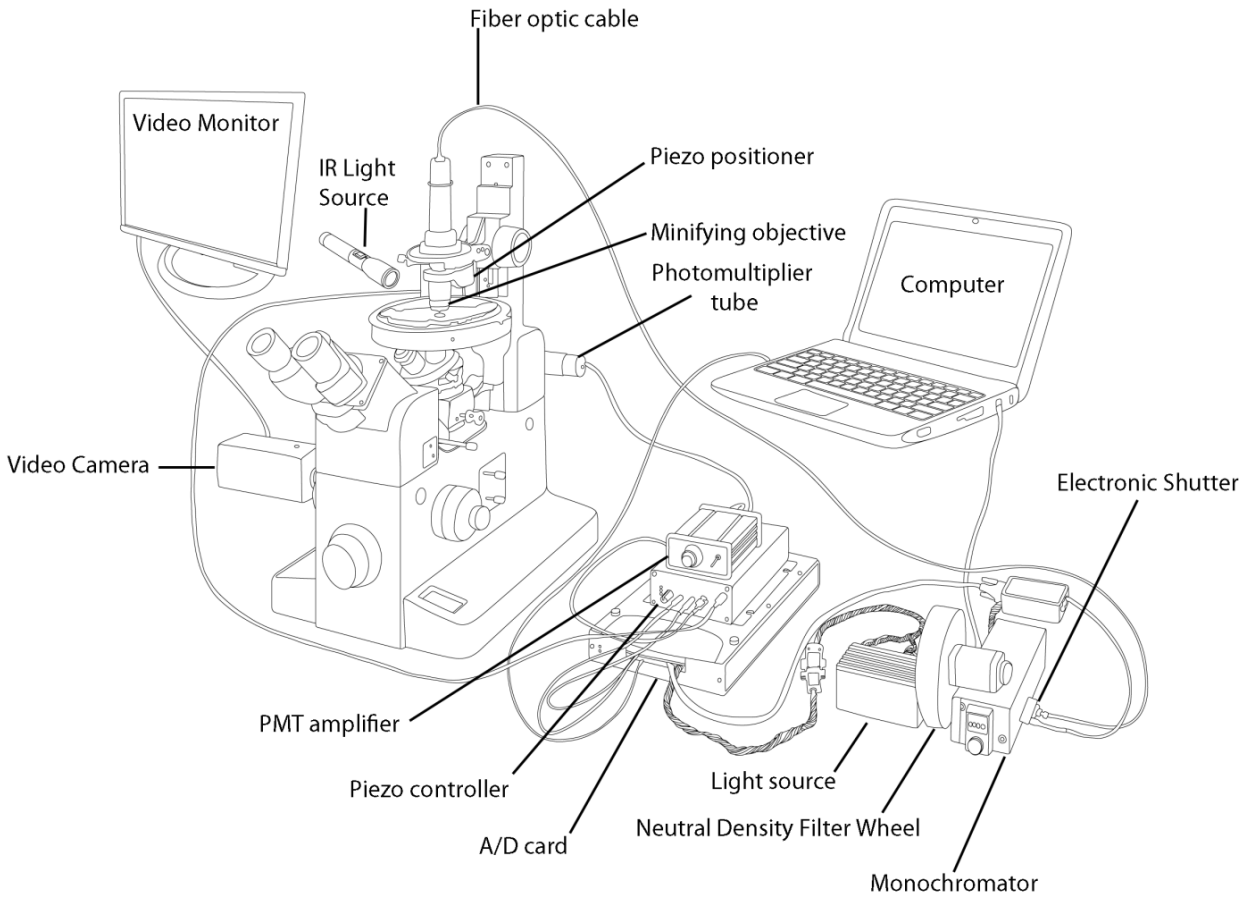

Figure S3, Related to Table 1 and Experimental Procedures. Diagram of the microspectrophotometer, computer, and microscope setup. Microspectrophotometry was performed using a custom-built apparatus. Broad-spectrum light emitted from a 20-watt quartz-tungsten-halogen source (Optometrics LLC, San Francisco, CA) was first passed through a motorized filter wheel (FW-103, Thorlabs, Newton, NJ) fitted with neutral density filters, and then through a scanning digital monochromator (SDMC1-02, Optometrics). The output was focused onto a 200 μm diameter UV-VIS transmissive fiber-optic cable (Ocean Optics). The image of the light exiting the fiber was then focused onto the sample using a UV-transmissive 32X microscope objective (Neofluar, Carl Zeiss Inc) forming a beam approximately 6 μm wide. A piezoelectric nanopositioner (86168 actuator with 12V40SG amplifier, Piezosystem Jena Inc., Jena, Germany) adjusted the focus as a function of wavelength to adjust for residual chromatic aberration. The focused spot was then imaged using an inverted microscope (Diaphot, Nikon Inc). The input voltage of the photomultiplier tube (PMT), the position of the filter wheel, and other parameters were adjusted using a custom-built virtual instrument programmed in Labview (National Instruments Inc., Austin, TX).

Spectra for dark, baseline, and sample recordings were taken from 300 to 800 nm and back again with a wavelength accuracy of 1 nm. Individual photoreceptors in the upward-facing and lateral-facing portions of the eye were scanned while fully dark adapted and the data was recorded. After initial recordings, photoreceptors were bleached with white light at one, five, ten, and 15 minute intervals to monitor the bleaching process, then re-scanned. Difference spectra were calculated by subtracting the 15 minute photobleached spectrum from the initial dark-adapted spectrum, which removes attenuation due to scattering and photostable pigments from the data. The long-wavelength limbs of the difference spectra (between 470 nm and 700 nm) were fitted to an A_1 rhodopsin template [S1] through a least-squared algorithm implemented using Solver (Excel 2010; Microsoft Inc., Redmond, WA, USA), which varied λ_{max}, peak height, baseline level, and optical path length. After fitting individual difference spectra to determine λ_{max}, peak values were averaged to find the mean λ_{max} of the *P. gracilis* photoreceptors.

Table S1, Related to Table 1. Morphological features of the bi-lobed eyes of *Paraphronima gracilis.* Mean, standard error of the mean (S.E.M.) and number of samples measured (n) are shown.

Feature	Mean (µm)	± S.E.M.	n
Dorsal Crystalline Cone Diameter	92	2	25
Dorsal Crystalline Cone Length	280	11	25
Dorsal Light Guide Length	1400	67	25
Lateral Crystalline Cone Diameter	67	2	25
Lateral Crystalline Cone Length	120	3	25
Lateral Light Guide Length	230	14	25
Rhabdom Width	12	1	100
Rhabdom Length	160	7	25

Supplemental References

1. Stavenga, D. G., Smits, R. P., & Hoenders, B. J. (1993). Simple exponential functions describing the absorbance bands of visual pigment spectra. *Vision Res.*, *33*(8), 1011-1017.